



The moths of extinction will eat  
my brain as they will my clothing,  
and it will all disappear.

Alina (Isobel) Hagan, MSc

Department of Physics

Lancaster University

A thesis submitted for the degree of

*Doctor of Philosophy*

November, 2023

The moths of extinction will eat my brain as they will my clothing, and  
it will all disappear.

Alina (Isobel) Hagan, MSc.

Department of Physics, Lancaster University

A thesis submitted for the degree of *Doctor of Philosophy*. November, 2023.

## Abstract

This is the beginning of the abstract that according to the regulations should not be any longer than 300 words. See point 9 in appendix 2 of the regulations <https://bit.ly/2Q4H43I>.

## Acknowledgements

Acknowledgements you may want to make. (this is not required when submitting your thesis before your viva and you can add a dedication in your final thesis after your viva if you wish.)

## Declaration

I declare that the work presented in this thesis is, to the best of my knowledge and belief, original and my own work. The material has not been submitted, either in whole or in part, for a degree at this, or any other university. This thesis does not exceed the maximum permitted word length of 80,000 words including appendices and footnotes, but excluding the bibliography. A rough estimate of the word count is:

Alina (Isobel) Hagan

## Publications

(This is an example taken from Andrew Moore's thesis, adapt this to suit your own thesis.)

**NOTE:** If you have done joint research e.g. whereby you are not the first author and you feel you need to state the contributions you have made in those papers that relate to your thesis then create another section like 'Contribution Statements' whereby you state your contributions in those papers that relate to the thesis. See Kelly Widdicks thesis (page 11) for a great example. If you do create a 'Contribution Statements' section that you may want to revise the your 'Declaration', of which Kelly Widdicks declaration is a good example. Kelly's thesis link <https://eprints.lancs.ac.uk/id/eprint/143606/1/2019widdicksphd.pdf>. Also for more details on the regulations by the university on declaring contribution statements see point 13 in appendix 2 of <https://www.lancaster.ac.uk/media/lancaster-university/content-assets/documents/student-based-services/asq/marp/PGR-Regs.pdf>

**ADDITIONAL NOTE:** If you have any papers under review perhaps speak with your supervisor before adding them here for anonymity reasons.

Only one publication, shown below, has been created directly from the thesis, from which large portions of this published work is used within chapter 3:

**moore-rayson-2018-bringing**

The following publication have been generated while developing this thesis, and to an extent has guided the thesis into what it has become:

**moss-etal-2019-fiesta**

moore-rayson-2017-lancaster

el-haj-etal-2016-learning

moore2016domain

# Contents

<b>1</b>	<b>Introduction</b>	<b>1</b>
1.1	Introduction . . . . .	1
<b>2</b>	<b>The ATLAS Experiment and The Large Hadron Collider</b>	<b>2</b>
2.1	Accelerators and Detectors: Basic Principles . . . . .	2
2.2	The Large Hadron Collider . . . . .	2
2.3	The ATLAS Detector . . . . .	5
2.3.1	Overview . . . . .	5
2.3.2	Coordinate system and common variables . . . . .	6
2.3.3	Inner Detector . . . . .	8
2.3.4	Calorimetry . . . . .	9
2.3.4.1	EM Calorimetry . . . . .	9
<b>3</b>	<b>BLS Trigger; Validation and Purity</b>	<b>10</b>
<b>4</b>	<b>Transverse Momentum Dependent Parton Distribution Functions and Quarkonium Production</b>	<b>11</b>
<b>5</b>	<b>Extraction of TMDs</b>	<b>12</b>
<b>6</b>	<b>Conclusions</b>	<b>13</b>
6.1	Results . . . . .	13
	<b>Appendix A Introduction</b>	<b>14</b>

A.1 Additional Tables . . . . .	14
<b>References</b>	<b>15</b>



# List of Tables

A.1 Caption . . . . . 14

# List of Figures

2.1	CERN Accelerator Complex schematic [1]. . . . .	3
2.2	Cross-Sectional slice of the ATLAS detector [2]. . . . .	5

# Chapter 1

## Introduction

### 1.1 Introduction

## Chapter 2

# The ATLAS Experiment and The Large Hadron Collider

### 2.1 Accelerators and Detectors: Basic Principles

### 2.2 The Large Hadron Collider

The Large Hadron Collider (LHC) is a modern proton-proton synchrotron located at the CERN complex, outside of Meyrin, Switzerland. At a circumference of approximately 27km the LHC is currently the largest particle accelerator on the planet, and similarly produces the highest centre-of-mass energies for  $pp$  collisions, reaching  $\sqrt{s} = 13\text{TeV}$ . The LHC was constructed from 1998-2008 in the tunnel previously occupied by the Large Electron-Positron Collider (LEP). It extends from from the CERN site, across the French border towards the Jura Mountains and round returning through Geneve and Meyrin. It is positioned on a plane inclined at 1.41% between 45-175 metres underground, a measure to protect both the experimental recordings from a large fraction of cosmic ray interference and the surface from any hazardous emissions from either the particle collisions or the synchrotron radiation.

The LHC is supported by a number of smaller accelerator systems designed

to provide proton bunches of the correct spacing and energy, these are visible in figure 2.1. The acceleration process begins with the injection of Hydrogen anions ( $H^-$ ) into LINAC<sup>1</sup>, which provides an acceleration to energies of 160MeV before the beam is passed on the Proton Synchrotron Booster (PSB)<sup>2</sup>. This continuous beam from LINAC is stripped of electrons and split consecutively amongst the four PSB rings, accelerated to 1.4GeV, and injected into the Proton Synchrotron (PS). PS produces bunches spaced by 25ns, accelerates these to 25GeV, and passes them over to the Super Proton Synchrotron (SPS) for the final energy increase up to 450GeV. Bunches inserted from SPS into the the LHC are brought from 450GeV

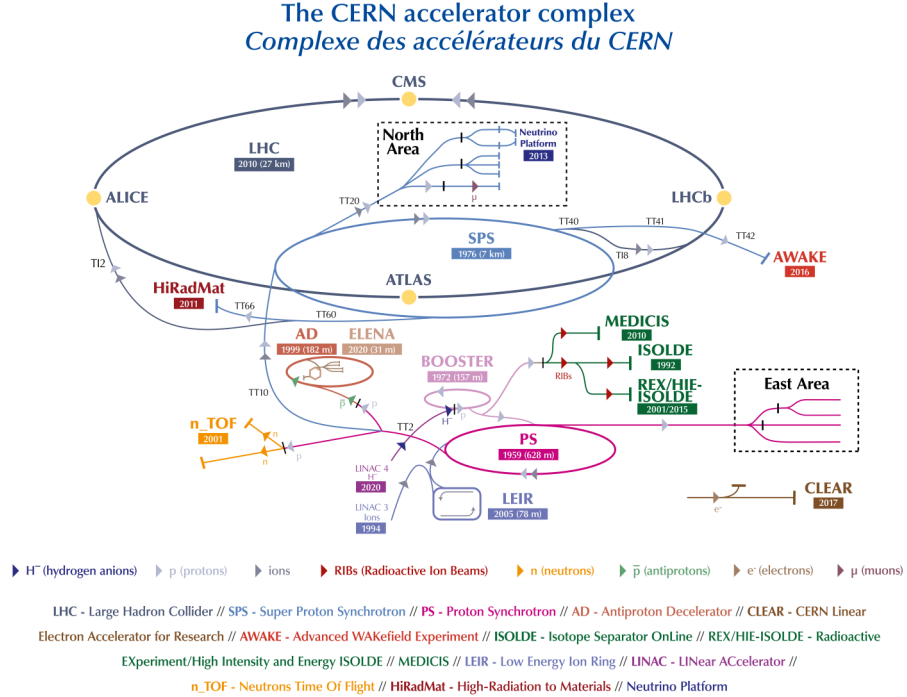


Figure 2.1: CERN Accelerator Complex schematic [1].

up to 6.8TeV over a timespan of approximately 20 minutes. This is driven by the 16 RF cavities around the LHC ring, oscillating at 400MHz each providing up to

<sup>1</sup>This was LINAC 2 until 2020, reaching 50MeV. During Long Shutdown 2 (LS2) this was obsolesced by LINAC 4

<sup>2</sup>idk psb

2MV of acceleration. The LHC beampipe is a dual-core design allowing bunches to travel in different directions allowing the CoM to coincide with the lab frame of a detector. For a single turn through the LHC, a proton bunch will pass through the magnetic field of 1232 superconducting dipole magnets. The magnets are of Niobium-titanite construction, are held at 1.9K, and produce a field of  $\sim 8.3\text{T}$ . In order to amplify luminosity at the interaction point a focussing effect is produced by the 474 quadropole magnets, arranged into FODO lattices positioned throughout the circumference.

There are 8 experiments that are part of the LHC, 4 of which are positioned around the circumference. These 4 are ATLAS, LHCb, CMS, and ALICE, located at points 1, 8, 5, and 2, respectively. These experiments are collectively engaged in Run 3 of the LHC. After commissioning and a magnet quench incident in 2008, the LHC entered full operation on 20 November 2009 with first collisions at 7TeV occurring on 30 March 2010. Run 1 concluded in early 2013, delivering a total integrated luminosity of  $22.8\text{fb}^{-1}$ . Run 2 began in 2015 and extended into 2018, raising the collision energy to 13TeV, and delivering a total of  $140\text{fb}^{-1}$ . After LS2<sup>3</sup> and the upgrades to both the LHC and detectors associated with this, the LHC began Run 3 operations with an increase in the collision energy, again, to 13.6TeV, and is currently ongoing in 2024. After Run 3, the LHC enters Long Shutdown 3 (LS3) for a series of upgrades to prepare for the HL-LHC phase where there is a roughly eight-fold increase in peak luminosity planned, and the total integrated luminosity over the HL-LHC period from Run 4 to the end of Run 6 planned in 2038 will be  $4000\text{fb}^{-1}$ .

---

<sup>3</sup>2018-2022

## 2.3 The ATLAS Detector

### 2.3.1 Overview

The ATLAS Detector[CITATION] as a general-purpose detector with cylindrical geometry and a forwards-backwards symmetry. It has nearly complete coverage, approaching  $4\pi$ , in solid angle around the interaction point (IP) which is located centrally within the detector layout. The detector is located at Point 1 on the LHC ring, approximately  $100m$  below the surface, with the ATLAS control room and supporting infrastructure located directly above at the Meyrin site of CERN. There

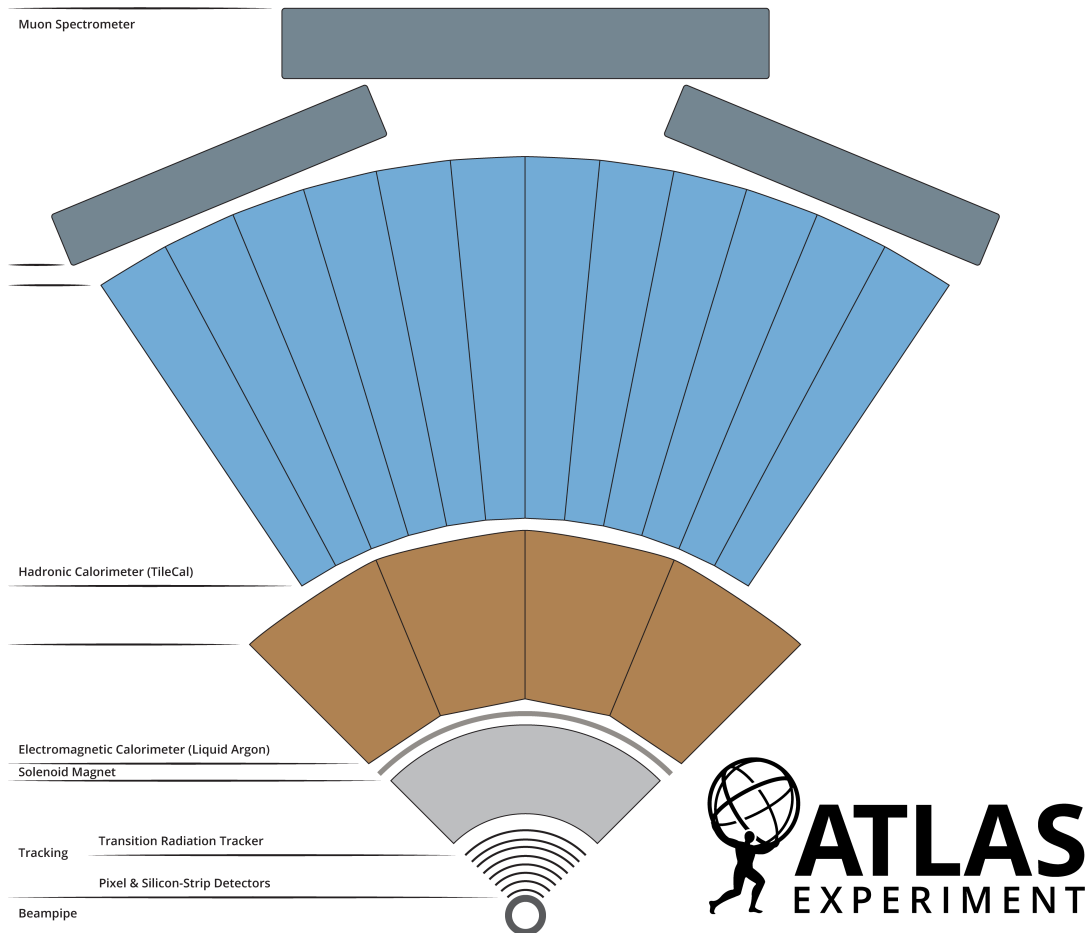


Figure 2.2: Cross-Sectional slice of the ATLAS detector [2].

are a number of main subsystems within the ATLAS detector, a cross-section of the detector outlining their positions is shown in 2.2 . Starting centremost radially, closest to the interaction point there is the Inner Detector (ID) comprised of the Pixel Detector, the Semi-Conductor Tracker (SCT), and the Transition Radiation Tracker (TRT). This is used to provide tracking information for all charged particles created in an event, a  $pp$  collision. The ID is immersed in a solenoidal magnet, producing a 2T field to generate a curvature in charged particle paths. Outside of this, the calorimeter systems begin with the Electromagnetic Calorimeter (ECal). The ATLAS ECal is a LAr Calorimeter in both the Barrel and Endcap Regions, and is used for precision measurement of Electron and Photon signals. The Hadronic Calorimeter (HCal) systems follow the ECal, these are designed for the measurement of strongly interacting particles which traditionally pass through the ECal and form showers further out from the interaction point. Three main components form the HCal, the Tile Calorimeter (TileCal) in the barrel region, and LAr calorimeters form the detector setup. in the endcap and forward regions. Last in the sequence are the Muon Systems (MS), placed in the outermost region to collect muons that typically penetrate through the earlier stages of the detector, or any other charged particles that may leak from the other inner stages. The MS is constructed from two main components in the barrel.

### 2.3.2 Coordinate system and common variables

To perform physics analysis at a  $pp$  experiment, several variables must be defined to accurately describe the physics objects that will be detected. The Cylindrical geometry of ATLAS lends towards using a cylindrical coordinate system for analysing events and is defined from a cartesian system centered around the interaction point. The  $x$ -axis points towards the centre of the LHC ring, the  $y$ -axis directly upwards, and the  $z$ -axis along the beamline. The Azimuthal angle  $\phi$  in this cylindrical system begins at the  $x$ -axis, and the polar angle  $\theta$  at the  $z$ -axis.

- **Energy  $E$ .** The energy of particles that are produced in reactions. This can



be assessed as the particle with deposit energy into the calorimeter materials as it travels outwards from the interaction point.

- **Transverse Momentum  $p_T$ .** This is the component of a particle momentum in the plane transverse to the beam line. In ATLAS this is used in preference to overall momentum on the basis that it is a conserved variable and is more informative of the physics given the typical kinematic distribution of events that would be expected in a  $pp$  collision of the nature at the LHC.
- **Invariant mass  $m$ .** Invariant mass can be used in the context of single particles or systems of them. Calculating the invariant mass of selected combinations of particles can yield information on the resonant particles within an event or interaction. This is typically calculated through combining information collected on the momentum and energy of a particle, or collection of particles.
- **Rapidity  $y$ , Pseudorapidity  $\eta$ , and Distance  $\Delta R$ .** These three variables help define a particle position after an interaction. Rapidity is an angular and relativistic measure of velocity, that can be used to define

$$y = -\frac{1}{2} \ln \frac{E + p_z}{E - p_z}.$$

Beneficially, rapidity differences are lorentz-invariant. When the particle masses are far smaller than the energy the rapidity can be approximated to the pseudorapidity, a more easily calculable and purely angular variable defined as

$$\eta = -\ln \tan \frac{\theta}{2}.$$

When combined with the azimuthal angle  $\phi$ , a lorentz-invariant distance measure appropriate for the cylindrical geometry can be defined;

$$\Delta R = \sqrt{\Delta\eta^2 + \Delta\phi^2}.$$

- **Tracking Parameters  $z_0$ ,  $d_0$ , and  $\frac{q}{p}$**  When combined with the beamspot position,  $\theta$  and  $\phi$ , these 5 variables are used to fully define a track in ATLAS.  $z_0$  is the longitudinal impact parameter, measuring the closest approach of the track to the beamspot along the axis of the beam,  $d_0$  distance of closest approach of a track to the beamline in transverse plane, and  $\frac{q}{p}$  is the charge-momentum ratio of a reconstructed track.
- **Transverse displacement  $L_{xy}$ , and lifetime  $\tau$ .**  $L_{xy}$  is the transverse displacement of a point, typically the vertex of a particle decay, from the beamline. Due to the relativistic nature of particles and the fact  $L_{xy}$  is not a variable natural to the rest frame of any decaying particle, it is preferable to use the pseudo-proper lifetime  $\tau$  in many cases;

$$\tau = \frac{L_{xy} m_{parent}}{c \cdot p_T}$$

### 2.3.3 Inner Detector

The ATLAS Inner Detector (ID), the first detector subsystem, provides the backbone of tracking and vertexing information for events recorded during LHC runs. Starting at a radius of 3.3cm the detector extends out to 1.05m and is 6.2m long. Innermost to this system, 3.3cm from the beamline, is the pixel detector (PIX/IBL), consisting of 4 layers of pixel layers, the innermost Insertable B-Layer (IBL) was installed in 2014. The IBL has a smaller pixel size, of  $50 \times 250\mu\text{m}$ , than the other pixel layers with  $50 \times 400\mu\text{m}$ , and was inserted to increase the tracking resolution of the ID. PIX/IBL provides 92 million readout channels, 12 million from the IBL alone, with a total  $1.9\text{m}^2$  of silicon area.

The second subsystem of the ID is the SemiConductor Tracker (SCT). As of Run 3 this is operating with 6.3 million readout channels consisting of silicon 'microstrips', in 4088 modules arranged across 4 barrel layers (2112 modules) and 18 endcap disks, nine each side ( $988 \times 2$ ), covering an area of  $60\text{m}^2$ . Detector planes are offset by 40mrad to assist in providing a readout accuracy as tight as  $25\mu\text{m}$ .

All modules in the barrel region are identical, they consist of four sensors paired off and connected back to back. Across the four sensors in a module there are 3072 readout strips (768 per sensor), pitched identically at  $80\mu\text{m}$ . The endcap modules have a variable micro-strip pitch dependent on their position as a function of their wedge-like geometry, though still have 768 readout strips per sensor.

The outermost section of the ID consists of the Transition Radiation Tracker (TRT). This is constructed from 300,000 thin-walled drift tubes of 4mm diameter with a total volume of  $12\text{m}^3$ . In the barrel region the straws are aligned parallel to the beam axis and extend from 560mm to 1080mm in radius. In the endcap region, the straws are aligned perpendicularly. Particle identification is performed with a combination of ionisation-loss curve analysis - CHECK, and using the probability of certain particles to produce readout pulses in the TRT that cross certain low and high eV thresholds, LT and HT respectively. The HT threshold for example is used for electron-pion discrimination.

### **2.3.4 Calorimetry**

The ATLAS calorimeter system is composed of two detector types, each type predominantly assigned to the two different tasks of Electromagnetic (ECal) and Hadronic (HCal) energy measurements. The LAr Calorimeter system consists of four components, the LAr Forward Calorimeter (FCal) for both ECal and HCal purposes, the LAr hadronic end-cap (HEC), the LAr electromagnetic end-cap (EMEC), and the LAr electromagnetic barrel. HCal in the barrel region is performed by the Tile Calorimeter (TileCal).

#### **2.3.4.1 EM Calorimetry**

## Chapter 3

# BLS Trigger; Validation and Purity

## Chapter 4

# Transverse Momentum Dependent Parton Distribution Functions and Quarkonium Production

## Chapter 5

### Extraction of TMDs

# Chapter 6

## Conclusions

### 6.1 Results

# Appendix A

## Introduction

### A.1 Additional Tables

Some extra tables A.1 that should go in the appendix.

5	6
7	8

Table A.1: Caption



# References

- [1] Ewa Lopienska. *The CERN Accelerator Complex, Layout in 2022. Complexe Des Accélérateurs Du CERN En Janvier 2022*. General Photo. 2022. (Visited on 08/23/2023).
- [2] Sascha Mehlhase. *ATLAS detector slice (and particle visualisations)*. 2021. URL: <https://cds.cern.ch/record/2770815>.